ELSEVIER

NeuroImage

www.elsevier.com/locate/ynimg
NeuroImage 38 (2007) 511–518

Myelination shapes functional activity in the developing brain

Eleonora Fornari,[a,*,1] Maria G. Knyazeva,[a,b,1] Reto Meuli,[a] and Philippe Maeder[a]

[a]*Department of Radiology, Centre Hospitalier Universitaire Vaudois (CHUV) and University of Lausanne, 1011 Lausanne, Switzerland*
[b]*Department of Neurology, Centre Hospitalier Universitaire Vaudois (CHUV) and University of Lausanne, 1011 Lausanne, Switzerland*

Received 21 February 2007; revised 25 June 2007; accepted 3 July 2007
Available online 24 July 2007

In humans, the function of spatial integration (SI) develops slowly, continuing through childhood into adolescence. To reveal its neural substrate in children and to examine the role of myelination in shaping SI-dependent functional activity, we applied a combined fMRI/MTI technique capable of tracking functional (BOLD response) and morphological (myelination) signs of maturation. Fourteen children (age 7–13) were scanned while viewing bilateral gratings, which either obeyed Gestalt grouping rules or violated them. A contrast between these stimuli revealed the BOLD response presumably induced by interhemispheric SI. It was limited to a small ventral stream territory in the *lingual gyrus* that corresponds to the VP part of the SI-induced activation found in adults in VP/V4 areas. The BOLD response correlated with myelination of splenial fibers. The data suggest that the activation of the extrastriate areas that enable an SI function depends on the maturation of long-range cortico-cortical connections.

Keywords: Children; fMRI BOLD; MTI; Myelination; Spatial integration; Splenium

Introduction

For many years myelination of the brain was viewed within the context of a purely biological ontogenesis. However, recently, intriguing evidence which links myelination to the environmental effects including cognition, learning, and social interaction has emerged in animal and human studies (reviewed by Casey et al., 2000; Paus, 2005; Fields, 2005). These findings prompted us to consider a relationship between myelination and the brain mechanisms of cognitive functions in human ontogenesis. To this end, the functions with protracted developmental trajectories susceptible to prolonged environmental influences are of primary interest.

Most of the visual functions achieve adult levels within a few months (e.g., contrast, motion and orientation sensitivity) or the first few years (grating acuity, binocularity) of postnatal life. In contrast, visual spatial integration (SI) develops slowly. SI refers to the processes that assemble local information across the visual field to implement a global representation of the spatially extended objects in the brain. Significant improvement in the performance of SI tasks such as contour integration, Glass patterns, figure-ground segmentation, and others (based on various cues) has been observed in children until mid-adolescence (Sireteanu and Rieth, 1992; Kovács et al., 1999; Atkinson, 2000; Norcia, 2003).

Animal models of SI suggest that the ability to integrate local elements depends on long-range interactions via horizontal cortical connections (Gilbert et al., 1996; Schmidt et al., 1997). Therefore, progressive myelination extending into early adulthood might affect SI-associated activity. To examine the role of myelination in shaping this functional activity, we applied a combination of two imaging methods. These are (*1*) the functional magnetic resonance imaging (fMRI) for localizing the neural substrate of SI in children and for measuring its activity, and (2) the magnetization transfer imaging (MTI) for determining the regional myelination of white matter.

We show the effects of myelination in the perceptual task of SI across visual fields. The information originating from the two hemifields is channeled to separate hemispheres and the fusion of the visual field relies on the callosal connections between visual cortical areas. The corpus callosum (CC) is a bundle of long-range fibers best studied in human ontogenesis. Different methods have provided converging evidence that the CC gradually myelinates during the first two decades of life (Yakovlev and Lecours, 1967; Rauch and Jinkins, 1994; Giedd et al., 1999; Thompson et al., 2000; Paus, 2005).

Recently we localized the neural networks associated with interhemispheric SI in adults (Knyazeva et al., 2006a). In these experiments, adult subjects viewed bilateral drifting gratings, which either obeyed Gestalt grouping rules (iso-oriented coherently drifting gratings, IG) or violated them (orthogonally oriented and drifting gratings, OG). Therefore, of the two stimuli, only IG was easily fusible into a single image across visual fields.

* Corresponding author. Fax: +41 21 314 44 88.
E-mail address: Eleonora.Fornari@chuv.ch (E. Fornari).
[1] EF and MGK contributed equally to this work.
Available online on ScienceDirect (www.sciencedirect.com).

1053-8119/$ - see front matter © 2007 Elsevier Inc. All rights reserved.
doi:10.1016/j.neuroimage.2007.07.010

Contrasting IG vs. OG in adults we demonstrated an increase in the BOLD signal associated with interhemispheric integration of the good-Gestalt stimulus within the fusiform and lingual gyri (VP/V4 areas). Since integrative functions of this area are well preserved in primates even across species, we expected to find similar localization of the area associated with SI in children and in adults. Furthermore, we hypothesized that the activation in this area induced by the good-Gestalt stimulus (IG) would correlate with the myelination of interhemispheric connections. Indeed, the BOLD response is proportional to local synaptic activity (Logothetis et al., 2001), which depends on the synchronization of the spike transfer along the CC axons (Cissé et al., 2004). In humans, the modulation of BOLD activation due to the distant EEG/MEG synchronization (Mizuhara et al., 2005; Knyazeva et al., 2006a,b; Winterer et al., 2007) matches the findings in animal models. Considering that the synchronization of an input depends on the axonal myelination, positive correlation might be expected between the BOLD response and regional myelination parameters.

Methods

Seventeen children without known neurological or psychiatric illness and with normal vision participated in the study. The study followed the protocol approved by the Lausanne University Ethics Committee and informed consent was obtained from children and their parents.

The protocol was performed on a 1.5-T Siemens Magnetom Vision. As a structural basis for brain segmentation and surface reconstruction, we acquired sagittal T1-weighted 3D gradient-echo sequence (MPRAGE, 128 slices, $1\times1\times1.25$ mm^3 voxels). It was followed by MTI and fMRI acquisition. The length of the recording session did not exceed 50 min. In younger children, if necessary, the MTI and fMRI sessions were performed on different days. We minimized head movements by placing the child's head on a vacuum beanbag. The high quality of individual MRI scans allowed an inclusion of data from 15 children (4 girls, 11 boys, mean age 10.5, range 7–13, SD 1.5 years) in the MTI analysis. The fMRI data from one of these children were removed from analysis because of artifacts induced by head motion, leaving a sample of 14 subjects for fMRI and joint MTI/fMRI analysis.

MTI

MTI estimates the efficiency of the magnetization exchange in biological tissues between a pool of free protons in intra- and extracellular water and a pool of protons bounded to macromolecules (Wolff and Balaban, 1989; McGowan, 1999; Eng et al., 1991, for review see Henkelman et al., 2001; Wozniak and Lim, 2006). Since lipid bilayers strongly bind protons, the extent, concentration, and integrity of myelin membranes are the most important contributors to the magnetization transfer effect. This two-compartment model of the MT effect fits experimental data. In particular, an *in vitro* study showed that the contribution of the myelin sheets to the MT contrast is nine times larger than the contributions of intra/extracellular water (Stanisz et al., 1999). Therefore, since the MT effect is mediated mainly through myelin-associated water, the MTI permits an accurate quantification of the myelination status of the brain.

This claim was validated by applying MTI to populations with known abnormalities in myelination, such as multiple sclerosis and Alzheimer's disease (Filippi et al., 1995; van der Flier et al., 2002; Rovaris et al., 1999; Kabani et al., 2002). Recently, the MTI method was successfully used in developmental studies as a stand-alone technique (Rademacher et al., 1999; van Buchem et al., 2001; Xydis et al., 2006).

We performed MTI by running a gradient-echo sequence twice; first with (M_S) and then without (M_0) an MT saturation pulse (FA 30, TE 15, matrix size 256×256, pixel size $1\times1\times3$ mm^3, 22 slices, MT pulse duration: 7.68 ms, FA 500, frequency offset 1.5 kHz). MT acquisitions were co-registered on the high-resolution T1 acquisition and a mask of segmented white matter was applied to both M_0 and M_S images. We calculated the magnetic transfer ratio (MTR) on a voxel-by-voxel basis as:

$$\mathrm{MTR} = [M_0 - M_S]/M_0{*}100$$

This value represents the percentage of signal loss caused by the transfer of magnetization from the bound saturated macromolecules to the free water pool of protons.

Regions of interest (ROIs)

The first ROI that we defined included the whole white matter volume. T1-brain images were automatically segmented into separate probability maps for grey matter (GM), white matter (WM), and cerebrospinal fluid (CSF) (Ashburner and Friston, 2000). Specifically, each intracranial voxel was classified as WM, or GM, or CSF, according to the outcome of a maximum likelihood procedure at its location. The entire WM binary mask was calculated from the resulting probability map (Fig. 1A).

Our second ROI contained visual interhemispheric connections, which go through the splenium of CC (Dougherty et al., 2005). According to the conventional partitioning scheme (for review see Zaidel et al., 1998), the splenium corresponds to the posterior 1/5 of the CC. It is separated from the rest of the CC by the borderline perpendicular to the line linking the most anterior and posterior points of the CC (Witelson, 1989). Therefore, technically the ROI was defined as the volume of white matter between two planes (Fig. 1B). The first plane cutoff the posterior 1/5 of the CC length perpendicular to the line representing maximum CC length. The second plane passed through the intersection between the first plane and the CC parallel to the same line.

To obtain general and regional characterizations of myelination for each child, we computed the mean MTR values across the total white matter volume and ROI (splenial system of fibers) volume ($\overline{\mathrm{MTR}}_t$ and $\overline{\mathrm{MTR}}_s$, respectively). Only voxels with MTR values exceeding 5% were considered to avoid the contamination of the data by noise.

For a comparison of the MTI results with the data reported in the literature, we also determined $\overline{\mathrm{MTR}}$ for the midsagittal area of total CC and of splenium and measured respective areas. The midsagittal slice was identified on the binary WM mask as the one containing a maximum sagittal CC area. We corrected for the head tilt by rotating the image, if this was necessary for providing more accurate midsagittal view of the CC. The splenium was defined as described earlier (Fig. 1D).

fMRI

During fMRI acquisition, subjects viewed black-and-white bilateral iso-oriented (IG) and orthogonally oriented (OG) sine gratings. IG consisted of two identical collinear, downward-drifting

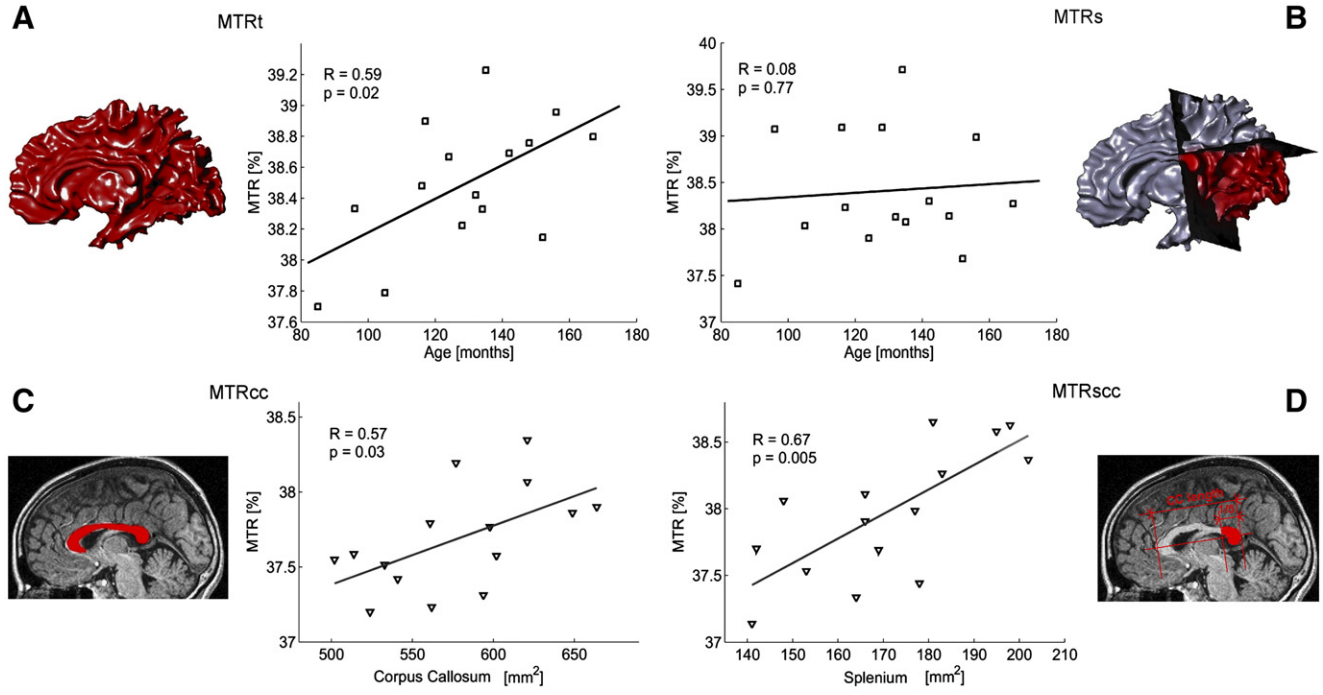

Fig. 1. Correlations of MTI myelination measures with age and morphometric measures. The correlations between $\overline{\mathrm{MTR}}$ and age for the total white matter $\left(\overline{\mathrm{MTR}_t}\right)$ are shown in panel A, for the splenial system of fibers $\left(\overline{\mathrm{MTR}_s}\right)$, in panel B. The bottom panels represent correlations between $\overline{\mathrm{MTR}}$ calculated for standard morphometric measurements of the CC and the splenium and respective areas. The correlations for the total midsagittal CC ($\overline{\mathrm{MTR}}$cc) are shown in panel C, and for the splenium ($\overline{\mathrm{MTR}}$scc), in panel D. Each plot includes the scatter diagram, the fitted first level polynomial, and the regression coefficient with P value. The ROIs are shown in red on the side of each plot. See Methods for detailed ROI definitions.

horizontal gratings on both sides of the fixation point. OG consisted of horizontal downward-drifting gratings on one side and vertical right-drifting gratings on the other side. The vertical and horizontal gratings of the OG stimulus appeared in the left or right hemifield in a random order.

All the gratings had a spatial frequency of 0.5 c/deg, a contrast of 70%, and a size of a lateral patch of 11° × 19° ($X \times Y$). They drifted with a temporal frequency of 2 Hz. A uniform grey screen served as a background. To compensate for retinal naso-temporal overlap and possible imperfect gaze fixation, all the stimuli were separated from the vertical meridian of the visual field by a 1° stripe of background on each side. Stimuli were displayed with an LCD projector at a refresh rate of 75 Hz. The projector was equipped with a photographical zoom lens projecting images onto a translucent screen in a custom-made mirror box positioned inside the magnet. The mirror box was designed to minimize light reflection. It allowed a subject to view the stimuli within the space defined by 25° horizontally and by 19° vertically.

We monitored gaze fixation with an eye tracking system (SensoMotoric Instruments GmbH, Teltow, Germany). The fixation stability was assessed as a percentage of time when the point-of-gaze was within a circle (Ø 2°) centered on the fixation point. Fourteen children, whose fMRI data are reported here, showed permanent fixation for 96–99% of the recording time.

Functional MRI images were acquired with an EPI gradient echo T2* weighted sequence (FA 90, TE 66, pixel size $3.75 \times 3.75 \times 5$ mm^3, acquisition time 1.7 s, 16 axial slices covering the whole brain) with a TR = 3 s and processed with SPM2. The protocol followed a block design in which the stimuli alternated with the background and each stimulus presentation lasted for 15 s. The stimuli were presented in a balanced randomized order 5 times for a total of 25 acquisitions for each condition. The whole recording session lasted 7 min 30 s.

Functional MRI acquisitions were rigidly realigned for motion correction, co-registered to the respective anatomical acquisition, normalized to the MNI template, and convolved with a Gaussian kernel (9 mm FWHM) in order to increase the signal-to-noise ratio. The fMRI data were analyzed according to the general linear model using a single-subject fixed-effects model, where the expected hemodynamic response was modeled by a canonical hemodynamic response function convolved with a square-wave function. We removed the signal drift across acquisitions by high-pass filtering and the global signal changes by proportional scaling. Due to the random presentation of the stimuli, the cut-off period of the high-pass filter varied between 180 s and 300 s. We modeled temporal autocorrelation with a first-order auto-regressive model.

For each contrast of interest of each subject, we computed the statistical parametrical maps as input values for the group statistics based on random field theory. The inferential statistics included T-tests for the contrasts IG (OG) > Background and IG > OG. Only clusters with the height threshold set at $P < 0.01$ and extended threshold $k > 30$ contiguous voxels corresponding to $P < 0.05$ (corrected) were considered significant. The group data were exported, denormalized, and displayed on a single subject's cortical flattened surface (Freesurfer software, http://surfer.nmr.mgh.harvard.edu). We identified the anatomical location of cluster boundaries and centers via transformation of MNI coordinates into Talairach space. Cluster positions were verified according to individual anatomical landmarks.

The MTR–fMRI BOLD correlation analysis

We analyzed the relationship between regional myelination ($\overline{MTR_s}$) and the fMRI BOLD response (IG>Background and OG>Background) with an across-subject ANCOVA. The ROI was defined by the extent of activation with the IG stimulus at $P<0.05$. The individual BOLD response (percent signal change) for each voxel within the ROI served as a dependent variable, $\overline{MTR_s}$ as a covariate, $\overline{MTR_t}$ and age as nuisance variables. In this way, we analyzed the relationship between the myelination of the splenial fibers and the local activation, excluding the contribution of global variation in myelination and of age across subjects.

Results

Myelination measures

We calculated a distribution of MTR percent changes for each child. From these individual distributions we extracted mean MTR values for the total white matter content ($\overline{MTR_t}$=38.51, SD=0.43, range=2.62, Fig. 1A) and for the region of splenial fibers ($\overline{MTR_s}$=38.48, SD=0.60, range=3.12, Fig. 1B). The MTR variability was similar to previous findings in children of the same age range (van Buchem et al., 2001).

We found a correlation between $\overline{MTR_t}$ and age (R=0.59, $P<0.02$, Fig. 1A). The increase in $\overline{MTR_t}$ as a function of age was estimated at 0.13% per year. A correlation of $\overline{MTR_s}$ with age turned out to be not significant (Fig. 1B). The $\overline{MTR_t}$ and $\overline{MTR_s}$ measures did not correlate.

For a better understanding of the progression of myelination as assessed by different techniques, we calculated the MTI myelination index for the midsagittal callosal area ($\overline{MTR}$cc, Fig. 1C) and for the midsagittal splenium area ($\overline{MTR}$scc, Fig. 1D) predominantly used to assess the development of myelination. We found a linear relationship between both MTI measures and the respective midsagittal callosal areas (Pearson's R_{cc}=0.57, $P_{cc}<0.03$; R_{scc}=0.67, P_{scc}=0.005, Figs. 1C and D).

Activation with fMRI BOLD

As followed from the IG>Background and OG>Background contrasts, the two stimuli activated similarly the striate and the extrastriate visual cortices in children (the extent of IG activation at $P<0.05$ is shown as the transparent dark yellow region in Fig. 3). Differential activation in the IG>OG contrast, significant at $P<0.05$ (corrected), was located in the *lingual gyrus* (Fig. 2, left). These two symmetrical clusters, centered on 10, −76, −6 (X, Y, Z) and on −18, −78, −14 (Talairach coordinates in the right and left hemisphere, respectively), were similarly extensive (k_r=95, k_l=88) and significant ($t_r>3.3$, $t_l>3.1$). A comparison with the adult group (Fig. 2, right; for details see Knyazeva et al., 2006a,b) shows that the good-Gestalt stimulus (IG) boosted activation in similarly located clusters, though they were more extensive in adults.

Regional myelination and fMRI activation

Finally, we addressed the main question behind this experimental design: is there a relationship between activation associated with the interhemispheric SI and the myelination of splenial fibers?

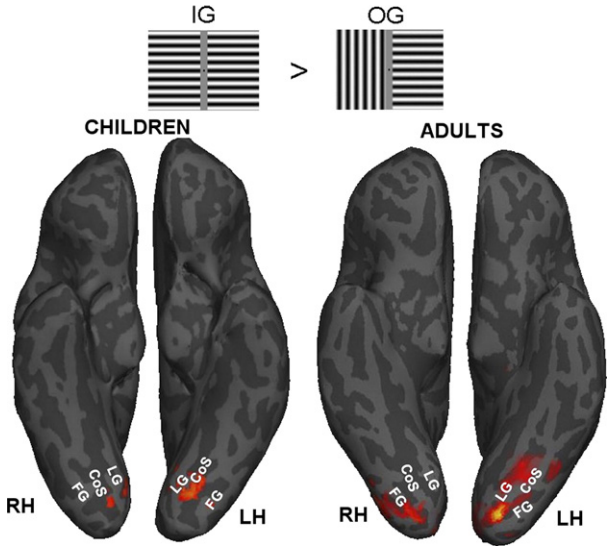

Fig. 2. The interhemispheric integration effects as revealed by the fMRI activation. Statistical maps of the IG>OG contrast (the stimuli are shown on top) for the children and adult groups are superimposed on individual inflated brains (bottom view). BOLD increase within and around the collateral sulcus is evident in both groups, but it is more extensive in adults (both maps were thresholded at $P<0.05$ (corrected)). The centers of the clusters are 30, −96, −3 (right) and −24, −87, −9 (left) for the adults, and 10, −76, −6 (right) and −18, −78, −14 (left) for children (Talairach coordinates). Hot scale represents P values. The sulci are presented in dark gray and the gyri in light gray. Anatomical labels: CoS, collateral sulcus; FG, fusiform gyrus; LG, lingual gyrus.

Specifically, we suggested that the BOLD response in the IG condition that allegedly involves interhemispheric SI would be facilitated by the myelination of splenial fibers, and, therefore, would correlate with the $\overline{MTR_s}$ within the integration areas. By contrast, the impact of the interhemispheric interaction on the BOLD response in the OG condition was expected to be a negligible one that would entail no correlations within the integration areas. Hence, out of the three contrasts described above, we used IG>Background and OG>Background to correlate with $\overline{MTR_s}$ values, and the differential contrast IG>OG to find out whether the correlation maps overlap the integration areas.

To this end, we performed an across-subject ANCOVA twice. Individual IG or OG activation maps served as a dependent variable, mean regional $\overline{MTR_s}$ as a covariate, and the mean $\overline{MTR_t}$ and age as nuisance variables. The analysis was performed on a voxel-by-voxel basis and was limited to the ROI defined by the extent of activation with IG stimulus at $P<0.05$ (Fig. 3). The ANCOVA performed on the IG activation maps revealed two clusters of voxels, in which BOLD response correlated with $\overline{MTR_s}$ ($P<0.01$, corrected at a cluster level). The clusters were symmetrically located in both hemispheres with the centers of gravity at 10, −80, −6 (right) and −12, −78, −10 (left). The correlation coefficients varied between 0.58 and 0.96 (mean=0.74, SD=0.09). Consequently, $\overline{MTR_s}$ explained between 33% and 92% of the variance of the BOLD response. As can be seen from the picture, these clusters covered a small area of the entire activated visual cortex. Specifically, only activation in the *lingual gyrus* was proportional to the myelination of the splenial system of fibers. A superposition of activation borders for the IG>OG

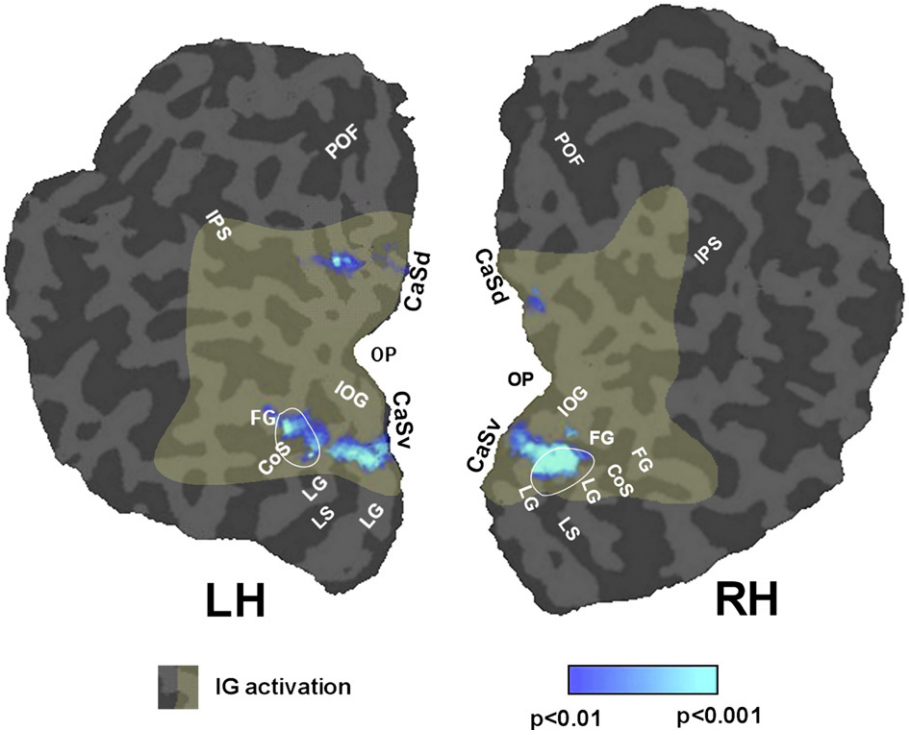

Fig. 3. Correlation between the BOLD response to the good-Gestalt stimulus (IG) and regional myelination. The ANCOVA results, denormalized according to individual inverse transformation, are superimposed on the flattened parieto-occipital cortex of the right and left hemispheres (LH and RH, respectively) of a single child's brain. The ROIs used to calculate correlations (see text for methods) are shown in transparent dark yellow. They include all the voxels in the visual areas activated at $P<0.05$ by the IG stimulus compared to the background. The map localizes the territory where the BOLD response is modulated by myelination of the splenial fibers (measured by $\overline{\mathrm{MTR}}_s$), within and around the *collateral sulcus*. Cold scale represents the significance of correlation. Note that only ventral clusters have survived the correction at a cluster level. The centers of these clusters are 10, −80, −6 (right) and −12, −78, −10 (left). The white contour shows the group activation border for the contrast IG>OG. Anatomical labels: CaSd, calcarine sulcus (dorsal part); CaSv, calcarine sulcus (ventral part), CoS, collateral sulcus; FG, fusiform gyrus; IOG, inferior occipital gyrus; IPS, intra-parietal sulcus; LG, lingual gyrus; LS, lingual sulcus; OP, occipital pole; POF, parieto-occipital fissure.

contrast (Fig. 3, white contour) clearly demonstrates that correlation maps overlap the areas preferentially activated by the good-Gestalt stimulus.

The same statistical test performed on the OG condition failed to show any voxels in which the BOLD response was significantly correlated with $\overline{\mathrm{MTR}}_s$.

To visualize our findings, we divided the whole group into two subgroups with 7 children in each one using $\overline{\mathrm{MTR}}_s$ as a selection variable (Fig. 4). The between-group difference in $\overline{\mathrm{MTR}}_s$ was significant at $P<0.001$ ($\overline{\mathrm{MTR}}_s$ high = 38.93 ± 0.18, $\overline{\mathrm{MTR}}_s$ low = 38.03 ± 0.25). At the same time, the subgroups were similar in terms of age and gender. In particular, both of them included 5 boys and 2 girls with the mean age of 10.8 ± 1.4 years in the subgroup with low myelination index, and of 11.1 ± 1.9 years, with high myelination index (Fig. 4A).

The children with immature interhemispheric connections (low myelination index) showed significant fMRI activation induced by SI (IG>OG) only in the left hemisphere (−14, −78, −14, $t>1.9$), while the children with relatively more myelinated posterior CC fibers showed a bilateral BOLD response (12, −80, −9, $t>2.9$ on the right and −15, −77, −11, $t>2.7$ on the left). In both subgroups, the *lingual gyrus* (VP) was involved, but the significance and the extent of activation appeared to approach the adults' pattern with myelination of the splenium (Fig. 4B).

Discussion

In children aged 7–13 years, we have localized the neural substrate underlying the function of SI to the *lingual gyri* in both hemispheres. Consistent with our hypothesis, we have shown that the intensity and extent of individual BOLD responses in these areas correlates with the myelination of the splenial system of fibers.

Since the retinotopic maps are similar in children and adults (Conner et al., 2004), we assume that in children the *lingual gyrus* corresponds to the VP area. This area belongs to the networks of the ventral visual stream related to perceptual categorization, object recognition, and contextual effects. A territory in adult brains with a similar location but much larger extension, covering both lingual and fusiform gyri (VP and V4), was activated by the same perceptual binding task (Knyazeva et al., 2006a,b).

Due to several potentially confounding factors, including excessive motion artifacts and immature attention in children, as well as dissimilar difficulty of the same task for children and adults, the between-group differences in the BOLD magnitude *per se* are not sufficient for establishing a developmental trend (for review see Stiles et al., 2003). Hence, albeit the observation of the delayed onset of a measurable activation response in the extrastriate V3/V4 areas of primates (Kourtzi et al., 2006) suggests that the maturation of extrastriate areas affects the BOLD response,

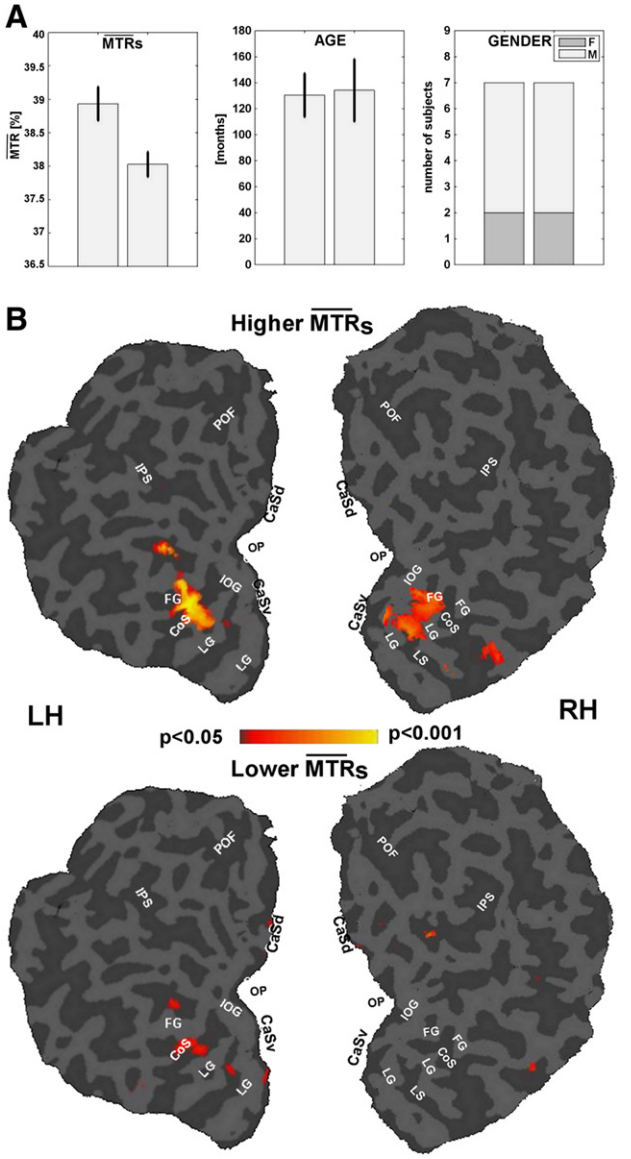

Fig. 4. The BOLD response to the interhemispheric integration task is linked to the state of regional myelination. (A) The children were divided into two groups according to the state of myelination of the splenial system of fibers (the between-group difference in $\overline{MTR}_s$ was at $P<0.001$). In each plot, the left bar stands for the data of a more mature group. Means and standard deviations for $\overline{MTR}_s$ and age are presented. The number of boys and girls was the same in both groups (5 and 2, respectively). (B) The IG>OG BOLD contrasts in children with a more mature (top) and less mature (bottom) myelination are shown on the same flattened brain surface as in Fig. 3. The maps show that, in children with immature connections, functional activation is more local and less affected interhemispherically. Hot scale represents P values. Anatomical labels are as in Fig. 3.

we avoid any direct comparisons between the two groups, using the adults' data only to show similar localization of the area activated by SI task. To reveal the developmental changes in functional activation, we focus here on the link between the BOLD signal and myelination in children.

The current understanding of the brain fibers' myelination during human ontogenesis has been dramatically enriched by *in vivo* imaging studies. In the repeatedly MRI-scanned children, a dynamic pattern of local growth rates with peaks and plateaus was revealed via tensor maps of the CC (Giedd et al., 1999; Thompson et al., 2000). Of special interest here is that, in contrast to the common belief that frontal areas of the brain have the longest developmental course, these authors reported a wave of growth spreading from rostral to caudal regions. The fastest growth of the posterior CC part was observed across the time span before and during puberty (6–13 years).

Consistent with the developmental trend, we found a linear relationship between age and the total white matter $\overline{MTR}$ in children aged 7–13. The estimated rate of the developmental change (0.13% per year) qualitatively agrees with the reported MTI data (Rademacher et al., 1999; van Buchem et al., 2001). However, intriguingly, there was no correlation between the regional $\overline{MTR}$ for the splenial system of fibers and age. The unexpected absence of the association motivated us to apply other (morphometric) measures of myelination reported in the literature and to test the relationship between the latter and our MTI estimations. To this end, we measured the midsagittal total CC and the splenium surface defined as in Giedd et al. (1999). In agreement with their evidence, we found a correlation between age and both total CC and splenium area (Fig. S1).

Moreover, we found a strong correlation between MTI measures and conventional morphometric measures of the CC and splenium. Since, for compatible ROIs, both methods resulted in coherent data, and the effects of age were confirmed by morphometric measures, their absence in the splenial system of fibers was unlikely due to the oddity of our sample, but probably stemmed from the properties of the ROI quantified.

Our ROI included the total length of fibers passing through the splenium. There exists evidence that myelination of the entire length of individual axons might be inhomogeneous (Friede and Hu, 1967). If this is true, the quantification of the regional myelination state must be more precise over such an ROI versus that over the midsagittal splenial area. Furthermore, the association of splenial volumetric measures with age has been obtained either in studies with a longitudinal design (Thompson et al., 2000) or over a longer developmental span including young children with the highest myelination rates (Giedd et al., 1999), which could have masked high interindividual differences in a shorter (pre) puberty period.

This variability cannot be attributed to the sex difference in brain maturation, since the subgroups of lower and higher myelinated children had the same gender composition (Fig. 4A). A likely source of the inter-individual differences could be the experience-dependent plasticity of myelination (Fields, 2005). Indeed, it has been shown recently that white matter maturation correlates with the development of motor skills, reading abilities, and various cognitive functions (Yurgelun-Todd et al., 2002; Nagy et al., 2004; Bengtsson et al., 2005; Schmithorst et al., 2005; also reviewed by Casey et al., 2000; Paus, 2005). Yet the mechanism that mediates this association remains unknown.

At a systems level, a missing link between myelination and cognitive functions is represented by the activity of their neural substrate. We come now to our central finding that the individual BOLD responses, induced in the ventral extrastriate areas, correlate with the myelination of the splenial system of fibers in children aged 7–13 years. The most impressive feature of the correlation maps (Fig. 3) is that, of the vast region activated by the good-Gestalt stimulus, the myelination index correlated only with the

voxels that responded to the IG > OG contrast and nearby ones, i.e., with the activity of networks presumably involved in the operations of SI.

The experiments with children reported here followed similar experiments with adults. In both studies we applied the same interhemispheric integration paradigm, but in adults the brain response was analyzed with a combined fMRI BOLD/EEG coherence technique (Knyazeva et al., 2006a,b). We demonstrated that, in adults, interhemispheric synchronization correlates with the activation of the same ventral areas sensitive to the operations of SI between visual fields.

In all probability, the synchronization of afferent input is regulated via myelination of long fiber tracts (Aboitiz et al., 1992). Since the BOLD response is proportional to synaptic activity, our evidence supports the hypothesis that the myelination shapes local synaptic activity via the synchronization of afferent input. Notably, in children, interhemispheric synchronization follows a developmental trajectory similar to the one shown for myelination (Farber and Knyazeva, 1993).

There exists another report pointing to the associated myelination of the long-range cortical connections and activation of their target areas in children aged 8–18 years (Olesen et al., 2003). The authors have found that the fMRI activation in the superior frontal sulcus and inferior parietal lobe was proportional to the myelination of fronto-parietal white matter. However, considering that both studies are based on a correlative approach, we cannot exclude other factors acting in concert with myelination such as sprouting up synaptic connections and/or branching neurons (Huttenlocher, 1979).

There are indications that perceptual mechanisms mediating contextual effects in pictorial illusions can be underdeveloped in children (Kovács et al., 1999). In light of the morpho-functional relationship described here, the inter-individual variability in the regional myelination might be to blame. Indeed, normal children of similar age might have variations in regional myelination, leading to a less efficient activation in immature children. Therefore, one can concede that myelination significantly impacts the shape of an individual developmental trajectory. Although this report presents only limited evidence for this hypothesis, this does seem to be a very fruitful direction for future research in developmental neuroscience.

Acknowledgments

This project was supported by Swiss National Science Foundation grant #3100A0-103993/1. We thank Ms. D. Polzik for assistance in the preparation of the manuscript.

Appendix A. Supplementary data

Supplementary data associated with this article can be found, in the online version, at doi:10.1016/j.neuroimage.2007.07.010.

References

Aboitiz, F., Lopez, J., Montiel, J., Aboitiz, F., Scheibel, A.B., Fisher, R.S., Zaidel, E., 1992. Individual differences in brain asymmetries and fiber composition in the human corpus callosum. Biol. Res. 598, 154–161.

Ashburner, J., Friston, K.J., 2000. Voxel-based morphometry—The methods. NeuroImage 11, 805–821.

Atkinson, J., 2000. The Developing Visual Brain. Oxford Univ. Press, USA.

Bengtsson, S.L., Nagy, Z., Skare, S., Forsman, L., Forssberg, H., Ullén, F., 2005. Extensive piano practicing has regionally specific effects on white matter development. Nat. Neurosci. 8, 1148–1150.

Casey, B.J., Giedd, J.N., Thomas, K.M., 2000. Structural and functional brain development and its relation to cognitive development. Biol. Psychol. 54, 241–257.

Cissé, Y., Crochet, S., Timofeev, I., Steriade, M., 2004. Synaptic enhancement induced through callosal pathways in cat association cortex. J. Neurophysiol. 92, 3221–3232.

Conner, I.P., Sharma, S., Lemieux, S.K., Mendola, J.D., 2004. Retinotopic organization in children measured with fMRI. J. Vis. 4, 509–523.

Dougherty, R.F., Ben-Shachar, M., Bammer, R., Brewer, A.A., Wandell, B.A., 2005. Functional organization of human occipital–callosal fiber tracts. Proc. Natl. Acad. Sci. U. S. A. 102, 7350–7355.

Eng, J., Ceckler, T.L., Balaban, R.S., 1991. Quantitative 1H magnetization transfer imaging in vivo. Magn. Reson. Med. 17, 304–314.

Farber, D., Knyazeva, M., 1993. Electrophysiological. correlates of interhemispheric interaction in ontogenesis. In: Ramaekers, G., Njiokiktjien, C. (Eds.), Pediatric Behavioural Neurology, Developing Brain and Cognition. Suyi Publ., pp. 86–99.

Fields, R.D., 2005. Myelination: an overlooked mechanism of synaptic plasticity? Neuroscientist 11, 528–531.

Filippi, M., Campi, A., Dousset, V., Baratti, C., Martinelli, V., Canal, N., Scotti, G., Comi, G., 1995. A magnetization transfer imaging study of normal-appearing white matter in multiple sclerosis. Neurology 45, 478–482.

Friede, R.L., Hu, K.H., 1967. Proximo-distal differences in myelin development in human optic fibers. Z. Zellforsch. Mikrosk. Anat. 79, 259–264.

Giedd, J.N., Blumenthal, J., Jeffries, N.O., Castellanos, F.X., Liu, H., Zijdenbos, A., Paus, T., Evans, A.C., Rapoport, J.L., 1999. Brain development during childhood and adolescence: a longitudinal MRI study. Nat. Neurosci. 2, 861–863.

Gilbert, C.D., Das, A., Ito, M., Kapadia, M., Westheimer, G., 1996. Spatial integration and cortical dynamics. Proc. Natl. Acad. Sci. U. S. A. 93, 615–622.

Henkelman, R.M., Stanisz, G.J., Graham, S.J., 2001. Magnetization transfer in MRI: a review. NMR Biomed. 14, 57–64.

Huttenlocher, P.R., 1979. Synaptic density in human frontal cortex–Developmental changes and effects of aging. Brain Res. 163, 195–205.

Kabani, N.J., Sled, J.G., Chertkow, H., 2002. Magnetization transfer ratio in mild cognitive impairment and dementia of Alzheimer's type. NeuroImage 15, 604–610.

Knyazeva, M.G., Fornari, E., Meuli, R., Innocenti, G., Maeder, P., 2006a. Imaging of a synchronous neuronal assembly in the human visual brain. NeuroImage 29, 593–604.

Knyazeva, M.G., Fornari, E., Meuli, R., Maeder, P., 2006b. Interhemispheric integration at different spatial scales: the evidence from EEG coherence and fMRI. J. Neurophysiol. 96, 259–275.

Kourtzi, Z., Augath, M., Logothetis, N.K., Movshon, J.A., Kiorpes, L., 2006. Development of visually evoked cortical activity in infant macaque monkeys studied longitudinally with fMRI. Magn. Reson. Imaging 24, 359–366.

Kovács, I., Kozma, P., Fehér, A., Benedek, G., 1999. Late maturation of visual spatial integration in humans. Proc. Natl. Acad. Sci. U. S. A. 96, 12204–12209.

Logothetis, N.K., Pauls, J., Augath, M., Trinath, T., Oeltermann, A., 2001. Neurophysiological investigation of the basis of the fMRI signal. Nature 412, 150–157.

McGowan, J.C., 1999. The physical basis of magnetization transfer imaging. Neurology 53, S3–S7.

Mizuhara, H., Wang, L., Kobayashi, K., Yamaguchi, Y., 2005. Long-range EEG phase synchronization during an arithmetic task indexes a coherent cortical network simultaneously measured by fMRI. NeuroImage 27, 553–563.

Nagy, Z., Westerberg, H., Klingberg, T., 2004. Maturation of white matter is associated with the development of cognitive functions during childhood. J. Cogn. Neurosci. 16, 1227–1233.

Norcia, A., 2003. Development of spatial selectivity and response timing in humans. In: Chalupa, L.M., Werner, J.S. (Eds.), The Visual Neurosciences. MIT Press, Cambridge, USA, pp. 1603–1615.

Olesen, P.J., Nagy, Z., Westerberg, H., Klingberg, T., 2003. Combined analysis of DTI and fMRI data reveals a joint maturation of white and grey matter in a fronto-parietal network. Brain Res. Cogn. Brain Res. 18, 48–57.

Paus, T., 2005. Mapping brain maturation and cognitive development during adolescence. Trends Cogn. Sci. 9, 60–68.

Rademacher, J., Engelbrecht, V., Bürgel, U., Freund, H., Zilles, K., 1999. Measuring in vivo myelination of human white matter fiber tracts with magnetization transfer MR. NeuroImage 9, 393–406.

Rauch, R.A., Jinkins, J.R., 1994. Analysis of cross-sectional area measurements of the corpus callosum adjusted for brain size in male and female subjects from childhood to adulthood. Behav. Brain Res. 64, 65–78.

Rovaris, M., Horsfield, M.A., Filippi, M., 1999. Correlations between magnetization transfer metrics and other magnetic resonance abnormalities in multiple sclerosis. Neurology 53, S40–S45.

Schmidt, K.E., Goebel, R., Löwel, S., Singer, W., 1997. The perceptual grouping criterion of colinearity is reflected by anisotropies of connections in the primary visual cortex. Eur. J. Neurosci. 9, 1083–1089.

Schmithorst, V.J., Wilke, M., Dardzinski, B.J., Holland, S.K., 2005. Cognitive functions correlate with white matter architecture in a normal pediatric population: a diffusion tensor MRI study. Hum. Brain Mapp. 26, 139–147.

Sireteanu, R., Rieth, C., 1992. Texture segregation in infants and children. Behav. Brain Res. 49, 133–139.

Stanisz, G.J., Kecojevic, A., Bronskill, M.J., Henkelman, R.M., 1999. Characterizing white matter with magnetization transfer and T(2). Magn. Reson. Med. 42, 1128–1136.

Stiles, J., Moses, P., Passarotti, A., Dick, F.K., Buxton, R., 2003. Exploring developmental change in the neural bases of higher cognitive functions: the promise of functional magnetic resonance imaging. Dev. Neuropsychol. 24, 641–668.

Thompson, P.M., Giedd, J.N., Woods, R.P., MacDonald, D., Evans, A.C., Toga, A.W., 2000. Growth patterns in the developing brain detected by using continuum mechanical tensor maps. Nature 404, 190–193.

van Buchem, M.A., Steens, S.C., Vrooman, H.A., Zwinderman, A.H., McGowan, J.C., Rassek, M., Engelbrecht, V., 2001. Global estimation of myelination in the developing brain on the basis of magnetization transfer imaging: a preliminary study. AJNR Am. J. Neuroradiol. 22, 762–766.

van der Flier, W.M., van den Heuvel, D.M.J., Weverling-Rijnsburger, A.W. E., Bollen, E.L.E.M., Westendorp, R.G.J., van Buchem, M.A., Middelkoop, H.A.M., 2002. Magnetization transfer imaging in normal aging, mild cognitive impairment, and Alzheimer's disease. Ann. Neurol. 52, 62–67.

Winterer, G., Carver, F.W., Musso, F., Mattay, V., Weinberger, D.R., Coppola, R., 2007. Complex relationship between BOLD signal and synchronization/desynchronization of human brain MEG oscillations. Hum. Brain Mapp. 28, 805–816.

Witelson, S.F., 1989. Hand and sex differences in the isthmus and genu of the human corpus callosum. A postmortem morphological study. Brain 112 (Pt 3), 799–835.

Wolff, S.D., Balaban, R.S., 1989. Magnetization transfer contrast (MTC) and tissue water proton relaxation in vivo. Magn. Reson. Med. 10, 135–144.

Wozniak, J.R., Lim, K.O., 2006. Advances in white matter imaging: a review of in vivo magnetic resonance methodologies and their applicability to the study of development and aging. Neurosci. Biobehav. Rev. 30, 762–774.

Xydis, V., Astrakas, L., Zikou, A., Pantou, K., Andronikou, S., Argyropoulou, M.I., 2006. Magnetization transfer ratio in the brain of preterm subjects: age-related changes during the first 2 years of life. Eur. Radiol. 16, 215–220.

Yakovlev, P., Lecours, A., 1967. The myelogenetic cycles of regional maturation of the brain. In: Minkrowski, A. (Ed.), Regional Development of the Brain in Early Life. Blackwell, Oxford, pp. 3–70.

Yurgelun-Todd, D.A., Killgore, W.D.S., Young, A.D., 2002. Sex differences in cerebral tissue volume and cognitive performance during adolescence. Psychol. Rep. 91, 743–757.

Zaidel, E., Iacoboni, M., Pacual-Leone, A.P., 1998. The Role of the Human Corpus Callosum in Sensory Motor Integration: Anatomy, Physiology, and Behavior; Individual Differences and Clinical Applications. Plenum Press, New York.